Fracture Toughness of Acrylonitrile-Butadiene-Styrene by *J*-Integral Methods

MING-LUEN LU, CHANG-BING LEE, *and* FENG-CHIH CHANG*

Institute of Applied Chemistry
National Chiao Tung University
Hsin-Chu, Taiwan, Republic of China

The fracture toughness of acrylonitrile-butadiene-styrene (ABS) was determined by three *J*-integral methods, ASTM E813-81, E813-87, and by hysteresis. The critical *J* values (J_{1c}) obtained are fairly independent of the specimen thickness, ranging from 10 to 15 mm. ASTM E813-81 and hysteresis methods result in comparable J_{1c} values, whereas the ASTM E813-87 was ~40% to 50% higher. The critical displacement determined from the plots of hysteresis (energy or ratio) and the true crack grow length vs. displacement are close. This indicates the critical displacement determined by the hysteresis method is indeed the displacement at onset of crack initiation, and the corresponding J_{1c} represents a physical event of crack initiation. The elastic storage energy, the input energy minus the hysteresis energy, is the most important factor in determining the onset of crack initiation. The critical elastic storage energy (at the beginning of crack growth) was found close to the J_{1c} obtained from the E813-81 or the hysteresis method.

INTRODUCTION

Before the development of fracture mechanics, yield stress or ultimate tension strength with a certain safety factor, was the conventional design criterion. Fracture mechanics addresses the situation where the presence of a flaw in the material causes fracture or failure when the conventional design criteria would deem the component as safe. Linear elastic fracture mechanics (LEFM), originally developed to characterize metals, has been successfully to describe fracture in many brittle polymers. Based on the principle of LEFM, fracture occurs when the magnitude of the stress intensity around the crack tip exceeds a critical value, K_{1c}. However, LEFM is not suitable for most rubber-toughened polymeric materials because of their relatively lower yield stress and significantly thicker specimen required to satisfy the size criterion.

The *J*-integral approach was proposed by Rice as a two-dimensional energy line integral that can be used as an analytical tool to characterize the crack tip stress and strain field under both elastic and plastic stress and strain (1). Begley and Landes applied the *J*-integral principle and developed a measurement of fracture toughness, J_{1c}, which represents the energy required to initiate crack growth (2, 3). Since then, two key ASTM standards, E813-81 and E813-87, have been established for *J*-testing, mainly for metallic materials (4, 5). These two ASTM-E813 standards have been used to characterize toughened polymers and blends during the last decade (6–24).

The J_{1c} definition has been confused and controversial, whether it is treated as crack initiation (ASTM E813-81) or is simply an engineering definition for design purposes (ASTM E813-87). Narisawa and Takemori studied several rubber-modified polymers and raised the questions on validity of the crack blunting line equation, since the blunting phenomenon was not being observed and the J_{1c} determined by E813-81 at the intersection point was higher than the real value corresponding to the actual subcritical crack growth directly observed on the polished side surfaces. They suggested that the true J_{1c} can be obtained by extrapolating the straight *R*-line to zero crack growth (25). Huang and Williams suspected the crack face may close as a result of plasticity-induced crack closure, obscuring any blunting of the crack tip (26, 27). Huang later studied *in-situ* SEM crack growth on rubber-toughened nylon 6,6 and observed crack blunting, but the growing process was not identical to that proposed for metals (27). Zhang *et al.* investigated the fracture toughness of ABS by plotting *J* vs. stress-whitening zone distance, and a transition of the plot was defined as J_{1c} (28).

*To whom correspondence should be addressed.

There is another class of integrity assessment procedure that disregards the initiation of ductile crack extension, but predicts the onset of unstable ductile crack extension occurring only after major crack growth (29, 30). Under this criterion, the physical interpretation of J_{1c} is not clear, as it does not represent the criterion for crack initiation.

When a precrack specimen of a toughened polymer is under load, viscoelastic and inelastic micromechanisms such as craze, cavitation, debonding, and shear yielding are expected to occur significantly around the crack tip region. These micromechanisms occur during the process of crack tip blunting (precrack) and during crack propagation. A portion of the storage energy is therefore consumed, and a relatively large crack tip plastic zone is formed, which can be quantified by the corresponding hysteresis energy. The crack tends to propagate within the plastic zone and results in the stable crack extension for rubber-toughened polymer materials.

In our studies on the fracture toughness of elastomer-toughened polycarbonate and high-impact polystyrene (HIPS), a new approach to the J-integral based on the above-mentioned hysteresis properties was proposed (31–34). The J_{1c} values obtained based on this hysteresis energy method are close to those from the ASTM E813-81 method, but are significantly lower than those from the ASTM E813-87 method.

THEORETICAL BACKGROUND OF J-INTEGRAL

A mathematical expression, a line or surface integral enclosing the crack front from one crack surface to other, has been used to characterize the local stress-strain field around the crack front. The fracture toughness can be expressed as follows:

$$J = \int_{\Gamma} \left(W dy - \bar{T} \frac{\partial \bar{U}}{\partial X} dS \right) \tag{1}$$

here $\bar{T}$ is surface traction, W is strain energy density, $\bar{U}$ is a displacement vector, and x, y are axis-coordinates. *Equation 1* is called the J-integral, which is path-independent. Physically, the J-integral can be considered as the difference of the potential energy between two loaded identical specimen with slightly different crack lengths, i.e.

$$J = -dU/B \cdot da \tag{2}$$

here B is the thickness of the loaded body, U is the total potential energy that can be obtained by measuring the area under the load-displacement curve (*Fig. 1*), and a is the crack length. This equation can be further expressed by following equation (35, 36),

$$J = J_e + J_p \tag{3}$$

here J_e and J_p are the elastic and plastic component of the total J value given by the following equations,

$$J_e = \eta_e U_e / B(W - a) \tag{4}$$

$$J_p = \eta_p U_p / B(W - a) \tag{5}$$

where U_e and U_p are the elastic and plastic components of the total energy. η_e and η_p are their corresponding elastic and plastic work factors. $(W - a)$ is the ligament length and W is the width. For a three-point-bend single-edge notched specimen with $a/W > 0.15$, η_p is equal to 2. When the specimen has a span of $4W$ ($S = 4W$) and $0.4 < a/W < 0.6$, η_e is equal to 2. Therefore *Eq 2* can be reduced to

$$J = 2U/B \cdot b \tag{6}$$

Equation 6 provides the basis for the determination of J_c by using the multiple specimen R-curve method.

In the ASTM E813-81 standard, the critical J value for crack initiation, J_{1c}, is determined by the intersection of the linear regression R-curve and crack blunting line, as follows:

$$J = 2m\sigma_y \cdot \Delta a \tag{7}$$

where σ_y is the uniaxial yield stress, Δa is the crack growth length, and m is a constraint factor ($m = 1$ for plane stress and $m = 2$ for plane strain). Two lines parallel to the crack blunting line at an offset of $0.006b$ and $0.06b$ (mm) are drawn, respectively, as the minimum and maximum crack extension lines.

In the ASTM E813-87 standard, instead of bilinear fit lines, the $J - \Delta a$ curve is then fit by a power law with the following equations,

$$J = C_1 \cdot \Delta a^{C_2} \tag{8}$$

$$\ln J = \ln C_1 + C_2 \cdot \ln \Delta a \tag{9}$$

The critical J value, J_{1c}, is now at the intersection of the power law fitted line and the 0.2 mm blunting offset line of the following equation,

$$J = 2\sigma_y \cdot \Delta a - 0.4\sigma_y \tag{10}$$

This construction indicates that the J_{1c} value must make the crack length grow to an additional 0.2 mm. The minimum and maximum offset lines are 0.15 mm and 1.5 mm parallel to the blunting line.

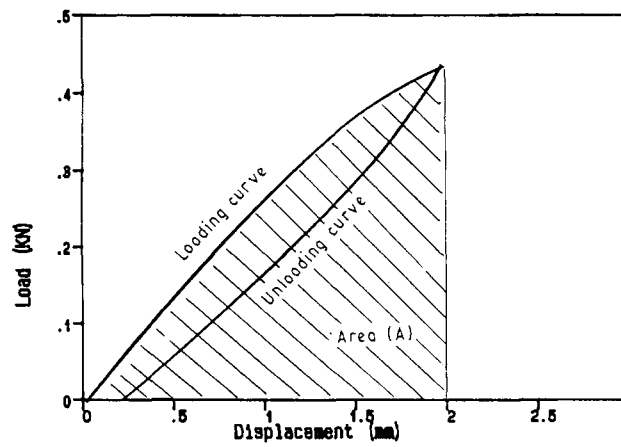

Fig. 1. A ASTM SENB loading-unloading curve, the hatched area, A, is used to approximate the J-integral, $J = 2A/B \cdot b$.

Hysteresis as defined in this method is not exactly the same as the conventional definition. It is the energy difference between the input and the recovery in the cyclic loading and unloading, which may include crack blunting and crack extension stages, as shown in *Fig. 1*. The close relation between the precrack hysteresis and the corresponding ductile-brittle transition behavior of polycarbonate and polyacetal has been reported (37–40). When a precrack specimen is under loading before the onset of crack extension (during blunting), a significant portion of the input energy is consumed and converted into a relatively larger crack tip plastic zone for the toughened polymers. These viscoelastic and inelastic energies may include many possible energy dissipated micromechanisms such as crazing, cavitation, debonding, and shear yielding, which can be related to the measured hysteresis energy. The hysteresis energy will increase gradually with the increase of load from the load vs. displacement curve. After the beginning of crack extension, the strain energy release due to crack growth will add to the observed total hysteresis energy. The rate of hysteresis energy increase, due to this strain energy release, is significantly higher than those above-mentioned precrack micromechanisms. Therefore, in a plot of hysteresis energy vs. deformation of a notched specimen, a clear transition from crack blunting to crack extension can be identified. Such a phenomenon, a drastic increase of the hysteresis energy immediately after the onset of the crack extension, can be used to determine the critical fracture toughness (J_{1c} value) as the onset of crack extension. The data observed to support this view point have been presented in our previous papers (31–34). The critical J value determined by this hysteresis energy approach, J_{1c}, has its physical meaning as the onset of crack extension rather than that based on the theoretically predicted blunting line as in ASTM E813-81 or that based on an arbitrarily chosen engineering definition as in ASTM E813-87.

EXPERIMENTAL

Cycolac ABS was obtained from GE Plastics. Specimens of three dimensions, 20 × 90 × 10 mm, 20 × 90 × 12.5 mm, and 20 × 90 × 15 mm, where prepared by injection molding using an Arburg injection molding machine. A starter crack of one-half the depth was created with a saw cutter and followed by sharpening with a fresh razor blade. The specimens were annealed at a temperature slightly higher than the T_g of the material for 2 to 3 h to release the internal stress prior to the bending testing. The J-method was carried out according to ASTM E813 at a crosshead speed of 2.0 mm/min by using an Universal tensile test machine, Instron model 4201. The crack growth length was measured at the center of the fracture surface by freezing the deformed specimen in liquid nitrogen and then breaking it open with a TMI impacter. The hysteresis energy was obtained by controlling the loading and unloading at the same test rate and then calculating the energy loss of the loading-unloading loop.

RESULTS AND DISCUSSION

J_{1c} Determination by ASTM Standards and Modified Versions

Multiple specimens were monotonically loaded and unloaded following the ASTM method, and the J values were calculated by using *Eq. 6* as shown in *Fig. 1*. The results from the specimen with $B = 15$ mm are summarized in *Table 1*.

Figure 2 shows the plot of the acceptable J vs. Δa by linear regression line according to ASTM E813-81. This linear regression intercepts with the blunting line (*Eq. 7*) to locate the J_{1c} value. The J_{1c} values obtained from E813-81 (*Table 2*) are generally independent of the specimen thickness if the specimen geometry is kept under a plane-strain condition. When the critical J value (J_0) is determined at the interception of the linear regression resistance curve with the Y-axis, as recommended by Narisawa and Takemori (25), the obtained J_0 is slightly lower (10–15%) than that determined by the E813-81 method, as would be expected.

In the ASTM E813-87 method, the J_{1c} is located at the intercept between the power law fit line and the 0.2-mm offset line, as shown in *Fig. 3* for $B = 15$ mm. The data obtained from ASTM E813-87 are summarized in *Table 2*. The power regressions of the data within exclusion lines (0.15 and 1.5 mm) give the following equations.

For $B = 10$ mm,

$$J = 282 \cdot \Delta a^{0.487}$$

For $B = 12.5$ mm,

$$J = 306 \cdot \Delta a^{0.482}$$

For $B = 15$ mm,

$$J = 187 \cdot \Delta a^{0.433}$$

The J_{1c} values obtained from the E813-87 method are ~40% to 50% higher than those obtained from the corresponding E813-81 method. The J_{1c} obtained from $B = 15$ mm is slightly lower than that from the

Table 1. Summarized J Data for ABS, $B = 15$ mm.

D mm	Input Energy, J	J KJ/m²	Hysteresis Ratio, %	Hysteresis Energy, J	Δa mm
1.2	0.10	1.37	4.0	0.004	—
1.4	0.14	1.81	3.0	0.004	0.025
1.6	0.17	2.31	4.5	0.0078	0.04
1.8	0.21	2.81	5.1	0.011	0.05
2.0	0.33	4.41	4.2	0.014	0.18
2.2	0.46	6.16	15.8	0.073	0.36
2.3	0.48	6.46	19.3	0.093	0.30
2.4	0.53	7.04	20.9	0.110	0.58
2.5	0.60	7.96	27.3	0.163	0.68
2.6	0.62	8.25	28.1	0.187	0.78

D: deformation displacement.
Δa: measured crack growth length.

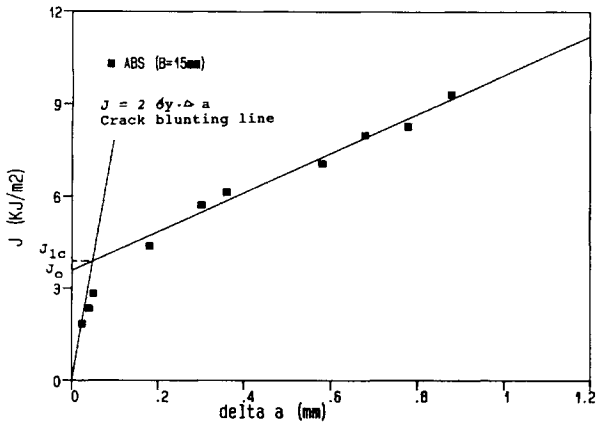

Fig. 2. J-Integral by ASTM E813-81 method.

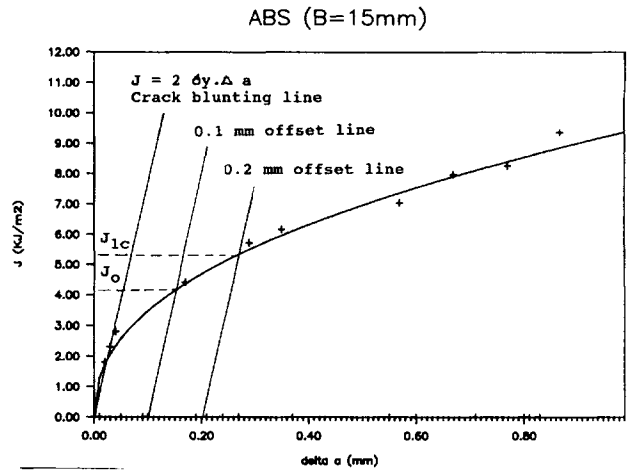

Fig. 3. J-Integral by ASTM E813-87 method.

Table 2. Summarized Data From Different *J*-Integral Methods.

ASTM E813-81 method			
	B = 10.0 mm	**B = 12.5 mm**	**B = 15.0 mm**
$J_{1c,81}$	4.01	3.95	3.95
$J_{0,81}$	3.56	3.56	3.57
dJ/da	7.23	7.50	6.35
ASTM E813-87 method			
	B = 10.0 mm	**B = 12.5 mm**	**B = 15 mm**
$J_{1c,87}$	5.81	5.95	5.31
$J_{0,87}$	4.45	4.54	4.18
dJ/da	11.49	12.16	10.13
Hysteresis energy method			
	B = 10.0 mm	**B = 12.5 mm**	**B = 15.0 mm**
Dc_1	1.80	1.84	1.89
J_{1c}	4.21	4.09	3.98
Dc_2	1.81	1.88	1.91
$dHE/B \cdot b \cdot da$	1.72	1.69	1.58

J unit: KJ/m^2
$J_{1c,81}$: from the standard ASTM E813-81 method.
$J_{0,81}$: from the modified version by intercepting with Y-axial.
$J_{1c,87}$: from the standard of ASTM E813-87 method.
$J_{0,87}$: from the modified version by using the 0.1 mm offset line.
Dc_1: critical initial displacement from the plot of hysteresis energy vs. displacement.
Dc_2: critical initial displacement from the plot of crack growth length vs. displacement.
$dHE/B \cdot b \cdot da$: hysteresis energy increase per crack growth area.

B = 10 mm and 12.5 mm. This is probably due to the relatively higher degree of plane strain of the thicker specimen. Only very limited comparative J_{1c} data between these two ASTM standards (E813-81 and E813-87) on polymeric materials have been previously reported. Huang (27) recently reported that the J_{1c} from the E813-87 method of the rubber-toughened nylon 6,6 is significantly higher than that from the E813-81 method (38 vs. 15 kJ/m^2). We also found that the J_{1c} values obtained from the E813-87 method for elastomer-modified polycarbonate (31) and high-impact polystyrene (33) are also about 20% to 40% higher than those from the E813-81 method. If the 0.2-mm offset line specified in E813-87 is now reset at 0.1 mm and the rest of the procedures are unchanged as shown in *Fig. 3*, the resultant J_{1c} obtained now becomes comparable to that from the E813-81 method (*Table 2*). Similar results were also obtained from elastomer-modified polycarbonate (31) and high-impact polystyrene (33). After all, the 0.2-mm offset line suggested in the ASTM E813-87 standard is only an arbitrarily selected value to define the critical fracture toughness (J_{1c}).

J_{1c} Determination by the Hysteresis Method

Figure 4 combines the plots of the hysteresis energy and J vs. crosshead displacement for the specimen B = 15 mm. The critical initiation displacement (Dc) is located at the intersection between the blunting line and the crack propagation line. As soon as the Dc is located, J_{1c} is determined from the plot of displacement vs. J curve. Since the measurement of crack growth is no longer necessary by this hysteresis energy method, it is relatively easier than the ASTM E813 methods. The J_{1c} values of ABS obtained from this hysteresis energy method are very close to those from E813-81 method, but still lower (40% to 50%) than those from the E813-87 method. *Table 2* summarizes the J_{1c} values of ABS, of three different thicknesses, obtained from this hysteresis energy method.

Figure 5 shows the plots of hysteresis ratio vs. crosshead displacement of ABS for the three different-thickness specimens. The critical displacement,

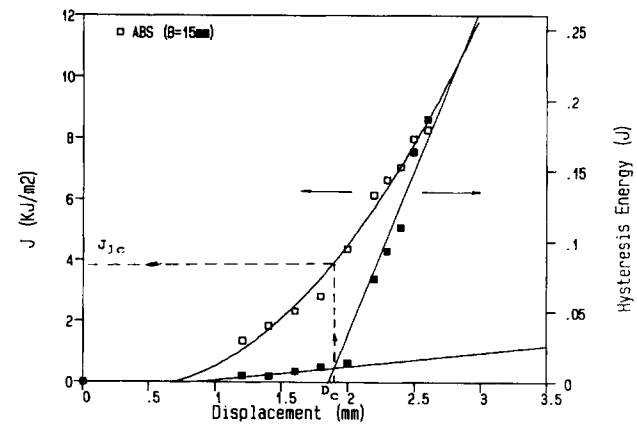

Fig. 4. J-Integral by hysteresis method.

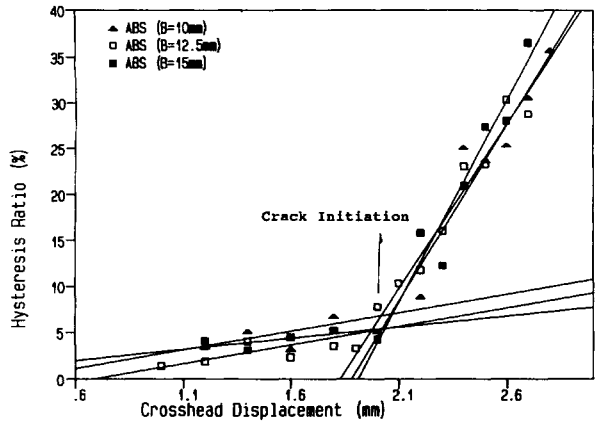

Fig. 5. The plots of hysteresis ratio vs. displacement.

intersection of the bi-linear lines, is assumed as the displacement due to the onset of crack initiation. The critical initiation displacements lie between 1.8 mm and 1.9 mm from these three different specimens. The plot of the crosshead displacement vs. crack growth length for $B = 15$ mm is shown in *Fig. 6*; the critical displacement is now located at the intersection between two linear regression lines. The critical displacements obtained are 1.81, 1.88, and 1.91 mm for $B = 10$, 12.5, and 15 mm, respectively. The critical displacements from these three methods, hysteresis energy vs. displacement, hysteresis ratio vs. displacement, and crack grow length vs. displacement, are fairly close. That means the critical displacement from hysteresis methods (energy or ratio) is indeed as the displacement due to the onset of crack extension.

The Size Criterion of Specimens

Paris *et al.* (12) developed the tearing modulus concept to describe the stability of ductile crack in terms of elastic-plastic fracture mechanics. This fracture instability occurs if the elastic shortening of the system exceeds the corresponding plastic lengthening for crack extension. A nondimensional parameter, tearing modulus (T_m), has been defined in *Eq. 11*:

$$T_m = (dJ/da)\left(E/\sigma_y^2\right) \tag{11}$$

where E, σ_y, and dJ/da are Young's modulus, yield stress, and the slope of resistance curve of the ASTM method. The dJ/da values obtained according to the linear regression R-curves of ASTM E813-81 are 7.23, 7.50, and 6.35 for $B = 10$, 12.5, and 15 mm, respectively. Similarity, the dJ/da values according to the power law regression curve of ASTM E813-87 at $\Delta a = 0.2$ mm are 11.49, 12.16, and 10.13 for $B = 10$, 12.5, and 15 mm, respectively. These comparative results indicate that the dJ/da values obtained from the E813-87 method are ~40% to 50% higher than those obtained from the E813-81 method (*Table 2*). The relatively lower dJ/da value obtained from the thicker $B = 15$ mm specimen is probably due to the higher degree of triaxial state than is found in the thinner specimens ($B = 10$, 12.5 mm). In order for the $J - \Delta a$ data to be regarded as an intrinsic material property independent of specimen size, the criterion of $\omega > 10$ must be met according to the following equation,

$$\omega = (dJ/da)[(W - a)/J_{1c}] \tag{12}$$

In this study, specimen dimensions employed meet the ASTM size criterion ($\omega > 10$), as shown in *Table 3*. The fracture toughness thus obtained (*Table 3*) is fairly independent of the specimen thickness ($B = 10$, 12.5, and 15 mm). According to ASTM E813 for J-testing, a valid J_{1c} value is obtained when the following size criteria must be satisfied,

$$B, (W - a), W > 25(J_{1c}/\sigma_y) \tag{13}$$

where B, W, and $W - a$ are specimen thickness, width, and ligament length, respectively. These size criteria produce a plastic plane-strain stress condition at the crack front and allow for the use of significantly smaller specimen dimensions than those required for LEFM testing. *Table 3* shows that the size criteria are met for all test specimens.

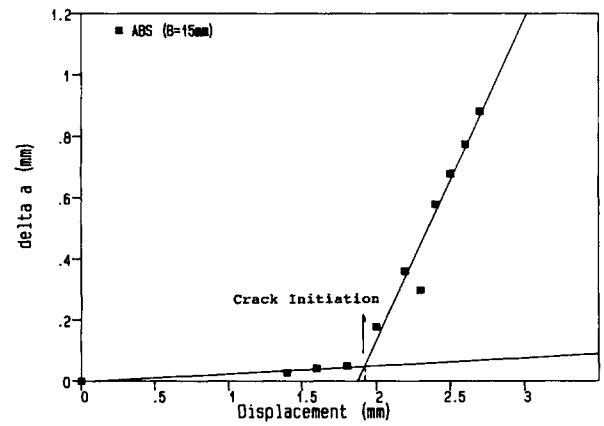

Fig. 6. Critical displacement determined by crack growth length vs. displacement.

FURTHER DISCUSSION

The load vs. displacement curve for $B = 10$ mm is shown in *Fig. 7*, where the experimentally obtained crack growth lengths (Δa) are labeled on the curve. The onset of crack growth in this load-displacement

Table 3. The Size Criterion of ABS Specimens.

	$B = 10$ mm	$B = 12.5$ mm	$B = 15$ mm
ASTM E813-81 Method:			
$25\ (J_{1c}/\sigma_y)$	2.50	2.47	2.47
ω parameter	18.30	18.98	16.08
$\omega > 10$	Yes	Yes	Yes
Plane strain	Yes	Yes	Yes
ASTM E813-87 Method:			
$25(J_{1c}/\sigma_y)$	3.63	3.72	3.32
ω parameter	24.45	20.43	19.07
$\omega > 10$	Yes	Yes	Yes
Plane strain	Yes	Yes	Yes

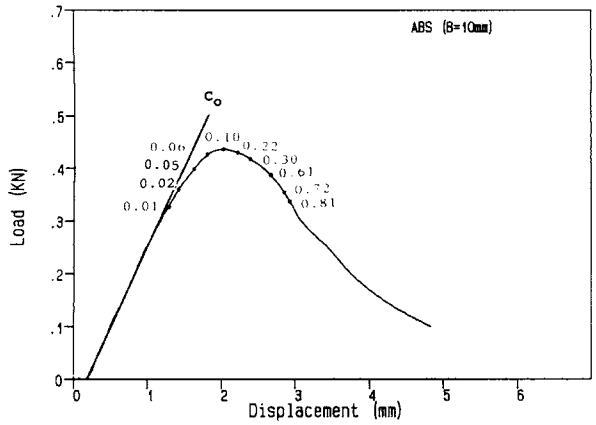

Fig. 7. The load-displacement curve showing crack growth lengths and elastic compliance determination.

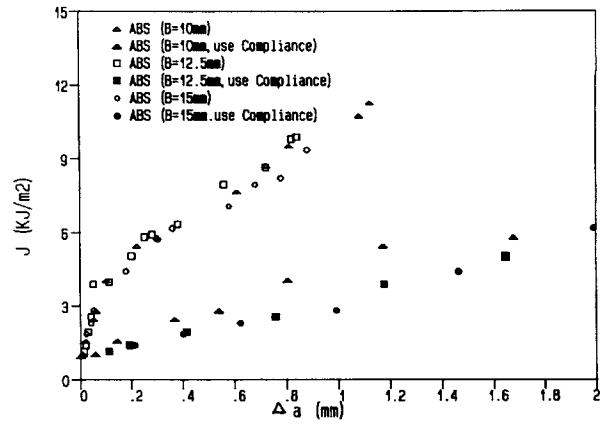

Fig. 8. Plots of J vs. Δa. Comparison between ASTM method and Eq. 16.

curve is located near the beginning of the nonlinearity of the curve. Analysis of the $J - \Delta a$ data using the LEFM theory by assuming no occurrence of plasticity in a specimen has been previously proposed. That means all the nonlinearity in the load-displacement curve is due solely to crack extension. In this situation, the Δa can be determined theoretically from a compliance measurement at any point along the load-displacement curve. The energy calibration factor, Φ, in an elastic body is given by

$$\Phi = (C/W)/(dC/da) \tag{14}$$

where C is the compliance of the body. For SENB specimens with $S/W = 4$, the $(1 - a/W)/\Phi$ is equal to 2. *Equation 14* becomes

$$da/(W - a) = 0.5\, dC/C \tag{15}$$

Integrating *Eq. 15* gives

$$\Delta a = (W - a_0)\left[1 - (C_0/C)^{1/2}\right] \tag{16}$$

where C_0 is the compliance at $a = a_0$. The Δa is calculated by using *Eq. 16* along the load-displacement curve shown in *Fig. 7* for specimen $B = 10$ mm. *Figure 8* shows Δa values calculated from *Eq. 16* and from the ASTM E813 method vs. corresponding J values. The calculated Δa values from *Eq. 16* are significantly higher than the actually measured values from fractured surfaces. The cause of the observed difference is the neglect of the plasticity under testing. The slopes of resistance curve from this compliance approach are lower than those from the standard ASTM E813-81 method (*Fig. 8*). Moskala studied core-shell rubber-modified polycarbonate by comparing ASTM E813-81 and the compliance approach and came to the same conclusions (42). This is not unexpected, since the compliance approach attributes all the nonlinearity to elastic crack extension.

The essential work theory proposed by Cotterell, Reddel, and Mai (43–46) was originally designed for plane stress ductile fracture. In a thin sheet of ductile polymer, the process zone is the necked-down region ahead of the crack tip. The total area under the load-deflection curve is defined as total fracture work, W_f. Cotterell and Mai (43–46) proposed that the W_f can be partitioned into the specific essential fracture work, W_e, and the inessential plastic work, W_p. In the analysis of fracture energy of a specimen by means of the hysteresis energy method, the total fracture energy W_t can also be partitioned into the hysteresis energy (W_h) during crack blunting and during crack extension and the recovery energy energy (W_r) (31–34, 37–40). The critical energy for crack initiation in elastic-plastic fracture has been found to be the elastic strain energy, the input energy minus the hysteresis energy, on the crack tip (37–40). Therefore, a tougher polymeric material can divert a larger fraction of the input energy into hysteresis energy and requires higher input energy to have the recoverable energy above the critical value for crack initiation. According to the LEFM theory, the strain energy loss is equivalent to the essential fracture work. *Figure 9* shows the plots of recovery strain energies (W_r) vs. crosshead displacements by linear regression lines that intercept the Y-axis to define the critical fracture toughness at the onset of initiation. The fracture toughness

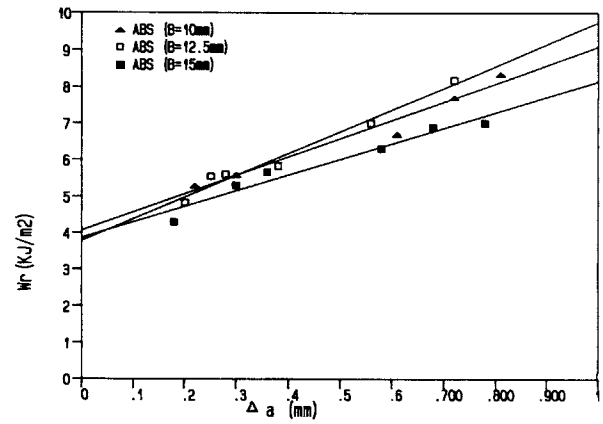

Fig. 9. The plots of recovery strain energy (Wr) vs. crack growth length.

thus obtained are 4.05, 3.78, and 3.86 kJ/m^2 for $B = 10$, 12.5, and 15 mm, respectively. These results are comparable to those obtained from the E813-81 method. This means that the most important factor in determining the onset of initiation is the elastic strain energy on the crack tip. It is interesting to note that this elastic strain energy matches closely with the J_{1c} obtained from E813-81 and the hysteresis energy method.

The implication of the sudden rise in the hysteresis ratio or hysteresis energy to crack initiation has its foundation as a physical event. The sudden increase of the hysteresis can be attributed to the potential energy release due to crack extension and new surfaces formed.

CONCLUSION

This hysteresis energy method is able to inherently adjust for the occurrence of crack blunting and thus avoid the controversy of the blunting issue. Besides, it is simple without the requirement of tedious crack growth length measurements. The J_{1c} values obtained from the hysteresis energy method are comparable with those from the E813-81 method but are ~ 40% to 50% lower than those from the E813-87 method. The J_{1c} values determined are independent of specimen thickness. The elastic strain energy, the input energy minus hysteresis energy, is the most important factor in determining the onset of crack initiation. When this elastic strain energy exceeds a critical value, crack extension starts. This critical elastic strain energy has been found to be close to the J_{1c} obtained form ASTM E813-81 and hysteresis energy methods.

ACKNOWLEDGMENT

This research project was financially supported by the National Science Council of Republic of China under contract number NSC 80-0405-E009-01.

REFERENCES

1. J. R. Rice, *J. Appl. Mech.*, **35,** 379 (1968).
2. J. A. Begley and J. D. Landes, *ASTM STP* **514,** 1 (1972).
3. J. D. Landes and J. A. Begley, *ASTM STP* **560,** 170 (1974).
4. ASTM Standard E813-81, in *Annual Book ASTM Standards*, Part 10, 822 (1982).
5. ASTM Standard E813-87, in *Annual Book ASTM Standards*, Part 10, 968 (1987).
6. A. P. Green and B. B. Hundy, *J. Mech. Phys. Solids*, **4,** 128 (1956).
7. G. Green and J. F. Knott, *J. Mech. Phys. Solid.*, **23,** 167 (1975).
8. G. A. Clarke, W. R. Andrews, P. C. Paris, and D. W. Schmidt, *ASTM STP* **590,** 27 (1976).
9. J. W. Hutchinson, *J. Mech. Phys. Solids*, **16,** 13 (1979).
10. C. F. Shin, H. G. Delorenzi, and W. R. Andrews, ASTM STP **668,** 65 (1979).
11. W. R. Andrews and C. F. Shin, ASTM STP **668,** 426 (1979).
12. P. C. Paris, H. Tada, A. Zahoor, and H. Ernst, ASTM STP **668,** 5 (1979).
13. J. R. Rice and G. F. Rosengren, *J. Mech. Phys. Solids*, **16,** 1 (1968).
14. M. K. V. Chan and J. G. Williams, *Int. J. Fract.*, A, **19,** 145 (1983).
15. S. Hashemi and J. G. Williams, *Polym. Eng. Sci.*, **26,** 760 (1986).
16. D. D. Huang and J. G. Williams, *J. Mater. Sci.*, **22,** 2503 (1987).
17. P. K So and L. J. Broutman, *Polym. Eng. Sci.*, **26,** 1173 (1986).
18. E. J. Moskala and M. R. Tant, *Polym. Mater. Sci. Eng.*, **63,** 63 (1990).
19. C. M. Rimnac, T. M. Wright, and R. W. Klein, *Polym. Eng. Sci.*, **28,** 1586 (1988).
20. I. Narisawa, *Polym. Eng. Sci.*, **27,** 41 (1987).
21. D. S. Parker, H. J. Sue, J. Huang, and A. F. Yee, *Polymer*, **31,** 2267 (1990).
22. Y. W. Mai, B. Cotterell, R. Horlyck, and G. Vigna, *Polym. Eng. Sci.*, **27,** 804 (1987).
23. N. Haddaoui, A. Chudnovsky, and A. Moet, *Polymer*, **27,** 1337 (1986).
24. I. C. Tung, *Polymer Bul.* **25,** 253 (1991).
25. I. Narisawa and M. T. Takemori, *Polym. Eng. Sci.*, **29,** 671 (1989).
26. D. D. Huang and J. G. Williams, *Polym. Eng. Sci.*, **30,** 1341 (1990).
27. D. D. Huang, *Polym. Mater. Sci. Eng.*, **63,** 578 (1990).
28. M. J. Zhang, F. X., Zhi, and X. R. Su, *Polym. Eng. Sci.*, **29,** 1142 (1989).
29. M. E. J. Dekkers and S. Y. Hobbs, *Polym. Eng. Sci.*, **27,** 1164 (1987).
30. I. Narisawa and M. T. Takemori, *Polym. Eng. Sci.*, **28,** 1462 (1988).
31. C. B. Lee and F. C. Chang, *Polym. Eng. Sci.*, **32,** 792 (1992).
32. C. B. Lee, M. L. Lu, and F. C. Chang, *Polym. Mater. Sci. and Eng.*, **64,** 510 (1992).
33. C. B. Lee, M. L. Lu, and F. C. Chang, *J. Appl. Polym. Sci.*, **47,** 1867 (1993).
34. C. B. Lee, M. L. Lu, and F. C. Chang, *J. Chin. Inst. Chem. Eng.*, **23,** 305 (1992).
35. M. K. V. Chan and J. G. Williams, *Polym. Eng. Sci.*, **21,** 1019 (1981).
36. J. D. Sumpter and C. E. Turner, *Int. J. Fract.*, **9,** 320 (1973).
37. F. C. Chang and H. C. Hsu, *J. Appl. Polym. Sci.*, **43,** 1025 (1991).
38. F. C. Chang and M. Y. Yang, *Polym. Eng. Sci.*, **30,** 543 (1990).
39. F. C. Chang and H. C. Hsu, *J. Appl. Polym. Sci.*, **47,** 2195 (1993).
40. F. C. Chang and H. C. Hsu, *J. Appl. Polym. Sci.*, to appear.
41. J. J. Strebel and A. Moet, *J. Mater. Sci.*, **27,** 2981 (1992).
42. E. J. Moskala, *J. Mater. Sci.*, **27,** 4883 (1992).
43. B. Cotterell and J. K. Reddel, *Int. J. Fract. Mech.*, **13,** 267 (1977).
44. Y. W. Mai and B. Cotterell, *J. Mater. Sci.*, **15,** 2296 (1980).
45. Y. W. Mai and B. Cotterell, *Eng. Fract. Mech.*, **21,** 123 (1985).
46. J. Wu, Y. W. Mai, and B. Cotterell, *J. Mater. Sci.*, **28,** 3373 (1993).

Revised May 1994